Title
Surface Studies of Zinc Oxide Growth on Cu(110)

Journal
Surface science, 237

Authors
Fu, S.S.
Somorjai, Gabor A.

Publication Date
1990-04-01

LBL-29027
Preprint

Center for Advanced Materials

CAM

Submitted to Surface Science

Surface Studies of Zinc Oxide Growth on Cu(110)

S.S. Fu and G.A. Somorjai

April 1990

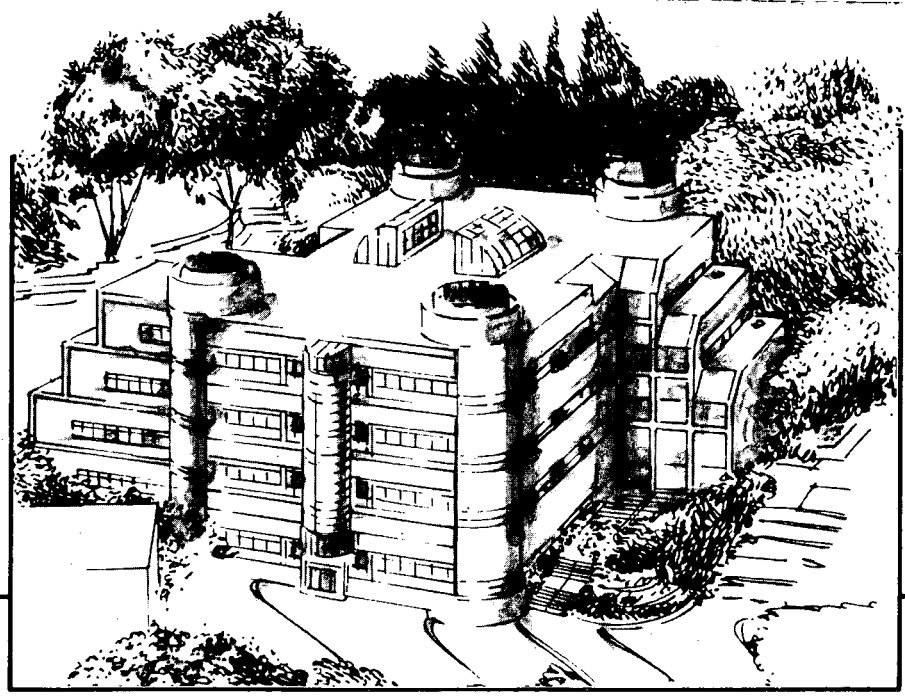

Materials and Chemical Sciences Division

Lawrence Berkeley Laboratory • University of California

ONE CYCLOTRON ROAD, BERKELEY, CA 94720 • (415) 486-4755

Prepared for the U.S. Department of Energy under Contract DE-AC03-76SF00098

DISCLAIMER

LBL-29027

Surface Studies of Zinc Oxide Growth on Cu(110)

S.S. Fu and G.A. Somorjai

Department of Chemistry
University of California

and

Center for Advanced Materials
Materials and Chemical Sciences Division
Lawrence Berkeley Laboratory
University of California
Berkeley, CA 94720

This work was supported by the Director, Office of Energy Research, Office of Basic Energy Sciences, Materials Sciences Division, of the U.S. Department of Energy under Contract No. DE-AC03-76SF00098.

Surface Studies of Zinc Oxide Growth on Cu(110)

by Sabrina S. Fu and Gabor A. Somorjai

Center for Advanced Materials
Materials and Chemical Sciences Division
Lawrence Berkeley Laboratory
1 Cyclotron Road
Berkeley, California 94720
and
Department of Chemistry
University of California
Berkeley, CA 94720

1 Abstract

Submonolayers to multilayers of zinc and oxygen deposited in UHV on Cu(110) were characterized by Auger Electron Spectroscopy(AES), Low Energy Electron Diffraction (LEED), and Temperature Programmed Desorption (TPD) of CO, CO_2, and zinc. Carbon monoxide adsorbs well on copper at 150K but only poorly on the oxides of copper and zinc. Carbon dioxide adsorbs on zinc oxide at 150K but not on copper or oxidized copper. We used a combination of CO and CO_2 adsorption to follow the initial growth of two-dimensional ZnO_x islands and the effect of heat and oxygen treatments on these two-dimensional islands. It is shown that heating above 300K leads irreversibly to three-dimensional island formation.

2 Introduction

Cu-Zn-O species are important as methanol synthesis catalysts. Hence, it is not surprising that several studies on the interaction of copper, zinc, and oxygen have been published [1-6], although none on the growth and characterization of submonolayers to multilayers of zinc and oxygen on copper single crystals. Campbell and co-workers[3] deposited copper on ZnO($000\bar{1}$) and characterized its growth by XPS, ISS, and LEED. These same researchers formed ZnO_x on Cu(111) by depositing in air, a droplet of ZnO-saturated water solution and then analyzed the resulting surface by XPS before catalytic studies. Chan and Griffin[5] examined the decomposition of methanol over copper deposited on oriented ZnO thin films, and found the properties of Cu/ZnO to be primarily a superposition of the separate copper and zinc oxide components. Didziulis and co-workers[6] performed a detailed surface science study of copper overlayers on ZnO(0001), ($000\bar{1}$), and ($10\bar{1}0$). Heating in UHV resulted in loss of copper XPS intensity which they interpreted as being due to three-dimensional clustering of the copper. They also found that copper deposited on Zn^{2+} terminated ZnO(0001) surfaces are most easily oxidized.

In this paper we present the results of our studies on the growth and chemical properties of the system formed when zinc vapor and oxygen are deposited onto copper single crystal surfaces of (110) orientation. The probes we used are AES, LEED, chemisorption of CO and CO_2, and Zn TPD. Carbon monoxide has been known to adsorb mainly on the copper part of reduced Cu-Zn-O catalysts[7], and this was confirmed by our studies of CO adsorption on Cu(110), Cu(110) with half a monolayer of oxygen overlayer (henceforth denoted 0.5ML O/Cu(110)), Zn, and ZnO_y. Carbon dioxide, on the other hand, adsorbs only on ZnO[8] and not on clean Cu(110)[9], or O/Cu(110), or Zn at 150K. By using selective CO and CO_2 adsorption to determine surface composition in Cu-Zn-O systems, we found rapid clustering of the initial two-dimensional ZnO_x islands above 300K.

3 Experimental

The experiments were performed in a stainless-steel ultra-high vacuum (UHV) chamber with a base pressure less than 2×10^{-10} Torr, pumped with an ion pump. The chamber is equipped with an off-axis Varian manipulator, a retarding field analyzer for low energy electron diffraction (LEED) and Auger electron spectroscopy (AES), and a UTI-100C quadrupole mass spectrometer for residual gas analysis and temperature programmed desorption (TPD).

The Cu(110) orientation single crystal was 99.999% pure, cut and polished by standard metallurgical techniques, and electrochemically etched in phosphoric acid. Disks 0.8 cm^2 were mounted with 20 mil platinum wires through 21 mil holes in the corners of the sample. This method gave uniform heating when resistively heated. Chromel-Alumel thermocouples made physical contact to the bottom of the sample in order to monitor temperature.

Zinc is deposited by evaporation of 99.999% pure zinc wires (Aldrich) enclosed in a Knudsen cell. This Knudsen cell is mounted in a stainless steel casing equipped with bellows and a shutter. In addition, the zinc source is equipped with water cooling capabilities and Chromel-Alumel thermocouples to monitor the temperature of the zinc. Unless otherwise noted, all zinc depositions are done in an ambient of 1×10^{-7}Torr O_2. Only zinc, oxygen, and copper could be detected by AES after zinc and oxygen depositions onto the copper.

Since the only non-overlapping zinc and copper AES peaks are at 918eV and 988eV (for ZnO_x), these peak intensities versus time, calibrated to CO_2 titration, were used to determine coverages.

The carbon dioxide (Matheson) was 99.99% pure with less than 0.1 ppm of carbon monoxide. The carbon monoxide (Matheson) used was 99.5% pure with less than 5 ppm of carbon dioxide. The oxygen (Matheson) used was 99.99% pure.

A typical experimental procedure is as follows: The copper single crystal is cleaned by cycles of sputtering with 5×10^{-5} Torr argon at 300K and 910K, and then annealed at

950K for fifteen minutes. Sample cleanness is then checked by AES and its structure by LEED. Once the sample is cleaned and the desired amount of zinc and oxygen deposited, TPD experiments begin. The sample is cooled to 150K, an AES spectrum is taken, the sample is positioned 2 mm in front of the mass spectrometer, dosed with a known amount of gas, and then the sample temperature is ramped linearly at 30 K/sec with the mass spectrometer tuned to a particular mass. AES spectra were obtained after each TPD experiment to correlate composition to CO and CO_2 TPD spectra. After characterizing each surface by AES, LEED, CO and CO_2 TPD, the sample temperature was ramped to $\approx$1100K while monitoring zinc, oxygen, or copper to further characterize these surfaces. All gases were checked for purity by the mass spectrometer. The residual background consisted of water, carbon monoxide, methane, helium, hydrogen, and argon, usually in that order of abundance adding to a total pressure of 2×10^{-10} Torr or less.

All CO and CO_2 TPD data presented in this paper were obtained from saturation coverages after dosing 2L of CO and 3L of CO_2 (without correction for ion gauge sensitivity).

Carbon dioxide TPD spectra were obtained at ten times the sensitivity scale relative to that used for carbon monoxide desorption spectra. All TPD data were collected using a 30K/sec linear ramp, and by monitoring $\frac{m}{e}$=44 for CO_2 and $\frac{m}{e}$=28 for CO.

For zinc TPD, $\frac{m}{e}$=64, corresponding to the most abundant zinc isotope, was used. Mass 63 was monitored to determine copper desorption. There is no natural isotope of zinc at this mass. For oxygen desorption, $\frac{m}{e}$=16 was used since there is contribution from zinc to $\frac{m}{e}$=32 signal but not to $\frac{m}{e}$=16 signal as determined by TPD of pure zinc from Cu(110).

Chemisorption studies on pure Zn were performed by depositing multilayers of the pure metal onto Cu(110). The term multilayers used throughout this paper means that enough material was deposited so that the substrate AES peaks at 918eV could not be detected. Chemisorption studies on submonolayers to multilayers of ZnO_y deposited on gold foils were performed to discern the relative role of copper compared to that of a more

inert metal.

To determine the chemisorption properties of oxidized copper, a Cu_xO surface was prepared by oxidizing a copper foil in 190 mTorr of O_2 at 470K for 30 minutes. This Cu_xO surface appears to be mainly Cu_2O as shown by the lack of satellite peaks in the copper 2p XPS spectrum (analysis done by air transfer to a PHI 5300 system).

The area under the peaks in the TPD spectra were used to determine the number of CO and CO_2 molecules adsorbed on our surfaces. The calibration was done by determination of the area under the CO desorption peak from a p(2×1) CO overlayer on Cu(110). This ordered structure corresponds to 0.5ML CO[10]. The amount of CO molecules desorbing from a p(2×1) CO overlayer was taken to be half the number of atoms on a Cu(110) surface. To determine the amount of CO_2, we took into account the mass spectrometer sensitivity to CO and CO_2.

The contribution from background desorption (from the Pt supports, etc.) of all three molecules was examined using a gold foil and was found to be non-detectable at the sensitivity scales used for CO and Zn TPD experiments, and contributed to ≈1% of the CO_2 TPD data.

4 Results

There are several difficulties in forming and studying zinc oxide overlayers on copper. We can see some of these difficulties when we examine and compare the interactions of the various two-component systems. For example, oxygen is readily dissociated onto Cu(110) at room temperature[11] and can dissolve into the bulk of copper[12]. In our laboratory, we have observed both the dissolution and segregation of oxygen on Cu(110). Not only does oxygen readily dissolve into copper, but so does zinc. Hence, we have the possibility to have both zinc and oxygen dissolved in copper. Zinc can be oxidized in the presence of O_2, but the dissociation of oxygen on zinc is a slow process relative to the dissociation of oxygen on Cu(110). In addition, the oxidation of zinc occurs via three-dimensional zinc oxide island formation surrounded by elemental zinc[13,14]. Figure 1 shows schematically

the different possibilities for zinc oxide growth on Cu(110).

Although figure 1 creates a very complicated picture of the Cu-Zn-O system, we will see that by combining several surface sensitive probes, we can understand what occurs upon deposition of zinc and oxygen onto Cu(110) and the effects that heat and further oxygen treatment has on these surfaces. In order to comprehend the three-component system of copper, zinc, and oxygen, an understanding of simpler one and two-component systems must be known. The first two subsections are devoted to present the results of several one and two component systems.

4.1 CO and CO_2 Chemisorption Properties on Cu, O/Cu, Cu_xO, Zn, and ZnO

Table 1 summarizes the chemisorption properties of CO and CO_2 on Cu(110), 0.5ML O/Cu(110) (0.5ML O/Cu is defined by a sharp p(2×1) LEED pattern [11]), oxidized copper, zinc, and zinc oxide. On Cu(110), CO adsorbs readily at 150K giving a narrow desorption peak at T_p=218K, with a saturation coverage of 0.5ML CO. Carbon dioxide, on the other hand, does not adsorb on Cu(110) at 150K[9]. Exposing Cu(110) to oxygen decreases its CO adsorption capacity[15]. Molecular oxygen does not desorb below 1000K. With 0.5ML O/Cu(110), the saturated CO adsorption has decreased to <10% of that on clean Cu(110). Carbon dioxide does not adsorb onto the oxygen covered Cu(110) surface.

In addition to O/Cu(110), we examined CO and CO_2 chemisorption on a Cu_xO surface, prepared by bulk oxidation of a copper foil. This surface behaves similarly to that of 0.5ML O/Cu(110); it adsorbs <0.05ML CO and does not adsorb detectable amounts of CO_2 at 150K.

We examined CO and CO_2 adsorption on multilayers of zinc deposited onto both gold foil and Cu(110). In both cases, we observed no detectable adsorption of CO or CO_2 on zinc.

Finally, we examined the CO and CO_2 TPD spectra of ZnO_y on gold substrates. Saturated CO adsorption by multilayers of ZnO_y is less than 0.05ML with a desorption peak centered at $\approx$200K. In contrast, CO_2 adsorption is readily observed and reaches satura-

tion at about 2.5×10^{14} molecules/cm^2 (see experimental section for determination). This corresponds to a CO_2 coverage of $\theta \approx 0.23$ (θ=1 is defined as 1.1×10^{15} molecules/cm^2). The CO_2 desorption peak from submonolayers to multilayers of ZnO_y on gold is always centered at 340K and 175K, even after annealing to 1170K. This indicates that ZnO_y overlayers on gold substrates are stable even after exposure to such elevated temperatures.

4.2 LEED patterns

Oxygen on Cu(110) forms a sharp p(2X1) LEED pattern associated with 0.5ML oxygen[11]. But various domains of a p(2X1) pattern can be seen above a coverage of 0.2ML oxygen. No new LEED pattern could be seen upon the deposition of ZnO_x onto Cu(110). By comparing I-V curves of (1X1) and p(2X1) LEED patterns with and without ZnO_x on the surface we can show that all LEED patterns are due to long range order of either Cu(110) or O/Cu(110), and are not due to the ZnO_x overlayer.

4.3 Preparation and Thermal Stability of Oxidized Zinc Layers on Cu(110)

The oxidation state of zinc layers on copper depends upon the oxygen content of the surface. AES shows a peak at 988eV (Zn LVV) for all surfaces independent of the oxygen treatment condition (temperature and exposure) except for zinc on clean copper, in which case the LVV transition occurs at 992eV. (note: Although we cannot resolve the 988eV and 992eV peaks, we can detect the 4eV shift.) The shift in the LVV zinc transition is indicative of the oxidation of zinc, but is not a good indicator of the stoichiometry of the oxide. From the oxygen AES peak alone, we cannot distinguish between the oxygen associated with copper and that associated with zinc.

The stability of the zinc layers as a function of oxidation extent was studied by TPD and the results are shown in figure 2. Zinc was adsorbed at 300K under four different conditions; 1) on clean Cu(110), 2) on 0.5ML oxygen preadsorbed on Cu(110), 3) in an ambient of 1×10^{-7} Torr O_2, and 4) same as (3) with additional oxidation in 5×10^{-7} Torr O_2 for 20 minutes at 300K. Zinc desorbs from the surface in the range of 700K-1100K,

depending on oxidation treatments. It is interesting to note that the two highest zinc desorption peaks from ZnO_x/Cu(110) occur at about the same temperature as two of the zinc desorption peaks from ZnO(0001) surfaces[16]. No zinc could be detected by AES after each of our zinc TPD experiment. Only oxygen was left on the copper surface as detected by AES, except where pure zinc was deposited on clean Cu(110) (figure 2(i)).

Although the vast majority of zinc has desorbed by 1000K, oxygen and copper desorption from these Cu-Zn-O surfaces are not detected below 1000K. Both the copper and oxygen signal continues to rise from 1000K to 1100K, where the TPD experiments end. Only when the temperature of the crystal approaches the melting point of copper does oxygen desorb. This indicates that the species on these Cu-Zn-O surfaces decompose by desorption of $Zn_{(g)}$ atoms, leaving oxygen adsorbed on the copper surface and also absorbed into the bulk of copper. The absorption of oxygen into copper is clearly observed when >2ML ZnO_x is heated to 1000K. No O_2 desorption is detected by the mass spectrometer (and virtually no H_2O) and yet the AES oxygen signal decreases considerably (always down to $\approx$0.6ML oxygen) after heating the surface to 1000K.

4.4 Initial two-dimensional growth of ZnO_x and the effect of heat

Oxygen produces a sharp p(2×1) structure on Cu(110) after an exposure of $\geq$10L O_2 corresponding to a coverage of half monolayer. For exposures between 10L and >300L O_2 at 300K, the AES spectrum and LEED pattern do not change. In contrast, even a 3,000L O_2 exposure at 300K is not sufficient to form a uniform ZnO surface from Zn(0001) surfaces[13]. Since oxygen is much more readily dissociated on Cu(110) than on zinc, we began all our preparations of ZnO_x overlayers with 0.5ML O/Cu(110).

In figure 3(i), we plot AES signal intensities of copper, zinc, and oxygen versus zinc deposition time. Zinc was dosed in an ambient of 1×10^{-7} Torr O_2 onto a 0.5ML O/Cu(110) (p(2×1)) surface at 150K (the need for low temperatures will become clear later). The p(2×1) LEED pattern disappears after 10 minutes deposition time. From the plot of AES intensities versus deposition time, it is hard to determine the monolayer completion point.

A better determination is by CO_2 adsorption on each freshly prepared ZnO_x surface. This is shown in figure 3(ii). A plot of the amount of CO_2 at saturation adsorption versus deposition time indicates the ZnO_x monolayer is completed after 20 minutes deposition time. The attenuation of the copper signal from its clean value is 25%, which is approximately the expected reduction for 918eV electrons going through one monolayer.

Carbon monoxide and carbon dioxide TPD spectra from freshly prepared 1.0ML ZnO_x surfaces are shown in figure 4(i). These surfaces adsorb less than 10% of the amount of CO that can adsorb on clean Cu(110) surfaces (and has CO desorption peak at T_p=190K rather than T_p=218K), and adsorbs 6.3×10^{13} CO_2 molecules/cm^2. This indicates that at saturation $\theta \approx 0.06$ for CO_2 adsorption. A value of $\theta \approx 0.1$ was found for the saturation coverage of CO_2 adsorption on ZnO(000$\bar{1}$) surfaces[17]. The most strongly bound CO_2 molecules on these two-dimensional ZnO_x islands desorb at T_p=510K, 170K higher than CO_2 from ZnO_y overlayers on gold.

This initial ZnO_x overlayer on Cu(110) undergoes very drastic changes after heating to 700K. The new surface obtained after cooling to 150K does not adsorb CO_2, and CO adsorption is restored to 100% of clean Cu(110) capacity with the same temperature at peak desorption (T_p=218K) as CO from Cu(110). This is shown in figure 4(ii). At this point, LEED shows a diffuse (1×1) pattern. AES shows only a 20% loss in zinc and oxygen intensities after the heat treatment.

The effect of heat upon the two-dimensional ZnO_x overlayer has been studied in more detail by performing the following experiments: We deposited zinc and oxygen at 150K, and increased the temperature of the crystal to a particular value. We then examined first the CO and CO_2 adsorption capacity of the surface, and finally, we examined the zinc desorption spectrum. Each experiment required the preparation of a fresh surface since above 300K, the initial ZnO_x overlayer changes. A plot of the area of CO and CO_2 desorption peaks versus the pre-annealing temperature is shown in figure 5. The ability of ZnO_x overlayers to adsorb CO_2 decreases by 350K, and the ability to adsorb CO begins to increase, slowly first at 350K, and then rapidly above 500K. Both these changes, along

with no detectable desorption of zinc from the surface for temperatures $\leq$700K point to either clustering of the ZnO_x overlayer into three-dimensional islands or diffusion of ZnO_x into the copper single crystal.

If ZnO_x dissolved into the subsurface region of copper, further annealing at 670K would dissolve more of the ZnO_x into the bulk of copper, and hence, less zinc would be detected during zinc TPD. Figure 6 shows the resulting zinc TPD after a) 0.8ML ZnO_x, and b)-c) same as (a) but with the addition of annealing at 670K for 5 minutes (b) and 10 minutes (c). In all three cases, the amount of zinc desorbed remains the same within a 10% experimental error. This could only be true if the ZnO_x overlayer formed three-dimensional islands since increased ZnO_x dissolution into copper would result in smaller amounts of zinc desorption after annealing treatments. AES indicates that there may be further clustering of the ZnO_x islands as there is a 30-40% loss in zinc AES intensity after 5 minutes of annealing at 670K. There is no difference by AES between the 5 minutes and 10 minutes annealing treatments.

We have seen from zinc TPD and CO chemisorption that upon heating to 700K, the initial two-dimensional ZnO_x overlayer clusters to form three-dimensional ZnO_x islands. We believe that these ZnO_x islands are oxygen deficient due to the inability of these islands to adsorb CO_2. The detection limit of CO_2 by our mass spectrometer is about $2X10^{11}$ molecules which is about $\frac{1}{300^{th}}$ of the CO_2 adsorption capacity on the initial two-dimensional ZnO_x overlayer. Within this detection limit, we do not observe any CO_2 adsorption after annealing the initial surface (prepared at 150K) to $\geq$600K for a fraction of a second. This inability of ZnO_x islands to adsorb CO_2 may be due to a slight loss of oxygen during the clustering process. Cheng and Kung[18] have noted that reduced ZnO single crystals of $(10\bar{1}0)$ orientation do not adsorb CO_2. If it is true that these ZnO_x islands are unable to adsorb CO_2 because they are oxygen deficient, then adding oxygen should restore their CO_2 adsorption capability. We will see in the next section that this is indeed so.

4.5 Effect of further oxygen and heat treatments on three-dimensional ZnO_x islands on Cu(110)

We show in figure 7(i) the effect of treating oxygen deficient three-dimensional ZnO_x islands on Cu(110) with more oxygen. We took the surface described in figure 4(ii) (a surface seen by AES to contain zinc, oxygen, and copper, but shown by CO and CO_2 TPD to be predominately Cu(110)) and exposed it to $5X10^{-7}$ Torr O_2 for 10 minutes at 300K followed by annealing at 700K for 2 seconds. This treatment restores the ability of the ZnO_x islands to adsorb CO_2 (note the highest T_p is now at 550K) and decrease the CO adsorption capacity by $\approx$40%. This may be interpreted as the spreading of ZnO_x islands onto Cu(110) or oxygen incorporation into deficient ZnO_x islands and adsorption of some oxygen on Cu(110). We believe the latter case to be true as patches of diffuse p(2×1) domains appear on the surface after the oxygen and annealing treatments described above, indicating oxygen adsorption on Cu(110).

Another indication that the oxygen and annealing treatments restore oxygen to deficient ZnO_x islands is that of CO and CO_2 adsorption capacity with the annealing treatment as compared to no annealing treatment. If CO is dosed onto the surface after O_2 treatment, the CO adsorption capacity decreases by 95%. But with each TPD experiment, CO adsorption capacity increases (up to that shown in figure 7(ia)) as each TPD experiment effectively anneals the surface for a fraction of a second at 700K. In addition, these non-annealed oxygen treated surfaces exhibit increasing CO_2 adsorption capacity with each TPD (up to that shown in figure 7(ib)). All this indicates diffusion of oxygen from Cu(110) to the oxygen-deficient ZnO_x islands when the surface is heated to 700K, hence increasing both the CO and CO_2 adsorption capacity of the surface.

We can continue oxygen treatment by an additional 5×10^{-7} Torr O_2 exposure for 10 minutes at 300K. Carbon dioxide TPD indicates that the ZnO_x islands have remained unchanged, while the CO TPD indicates further oxygen adsorption on Cu(110). This is shown in figure 7(ii). Annealing this surface at 700K for a few seconds does not change the CO and CO_2 chemisorption properties. It is because the ZnO_x islands no longer need

oxygen that annealing at 700K for 2 seconds does not result in loss of oxygen from the copper to the ZnO_x islands.

Zinc TPD from these stable three-dimensional ZnO_x islands always contain the highest zinc desorption peak at $T_p \approx 1000K$ (the desorption is half order so it is hard to define one T_p). This is the main difference between the zinc TPD spectra from the oxygen deficient ZnO_x islands and these "stoichiometric" ZnO_x islands.

The hypothesis that the CO and CO_2 TPD spectra shown in figure 7(i) are due to ZnO_x islands on Cu(110) may be further tested by co-adsorption of CO and CO_2. If there are ZnO_x clusters on Cu(110), co-adsorption of saturation coverages of CO and CO_2 should have little or no effect on the adsorption capacity of CO and CO_2. Table 2 shows the amount of CO and CO_2 adsorbed on a "3.0ML ZnO_x" overlayer on Cu(110) (coverage determined by AES). From CO titrations, this surface has $\approx$70% of the copper surface area of clean Cu(110). No change in either CO_2 or CO adsorption capacity could be detected by co-adsorption of the two molecules, further indicating the model of three-dimensional ZnO_x islands on bare Cu(110).

We can obtain reproducible CO_2 and CO TPD spectra ending at 700K from these three-dimensional ZnO_x islands on Cu(110). But as TPD experiments are performed with a heating rate of 30K/second, each TPD only anneals the surface for a fraction of a second at 700K. If we anneal these Cu-Zn-O surfaces for longer periods of time, we see changes by AES, LEED, and CO and CO_2 TPD. The changes in CO_2 TPD spectra for a 3.0ML ZnO_x/Cu(110) surface are shown in figure 8 and all the changes observed are summarized in table 3. Carbon dioxide TPD spectra show changes in the ZnO_x overlayer from the heat treatments at 700K. A new peak at 340K appears and increases with annealing treatment. This indicates new adsorption sites for CO_2. But the total CO_2 adsorption capacity does not increase; on the contrary, it decreases slightly due to a decrease in the other types of adsorption sites. Auger indicates a loss in both zinc and oxygen intensity after annealing at 700K for 2.0 minutes. This is most likely due to additional clumping of ZnO_x islands. There are no changes in either CO adsorption or

in the LEED pattern after the 2.0 minutes annealing treatment. But after an additional 10.0 minutes of annealing at 700K, CO adsorption does decrease by 70%. This decrease in CO adsorption capacity is accompanied by a diffuse p(2×1) LEED pattern, indicating that the decrease in CO adsorption capacity is due to oxygen adsorption on Cu(110). The oxygen is believed to surface from the bulk of copper as the annealing is done in vacuum. Similar results were obtained for a wide range of ZnO_x coverages from 0.5ML to 3.0ML ZnO_x.

The heat treatments were performed in an attempt to spread the three-dimensional ZnO_x islands onto Cu(110). Since heating in vacuum failed to spread these islands, heating in oxygen was attempted; up to 5×10^{-8} Torr O_2 was used. There was no additional effect of the oxygen ambient other than to create an oxygen covered Cu(110) surface more rapidly.

We can continue to deposit zinc and oxygen and obtain approximately the same CO_2 and CO adsorption capacity (9×10^{13} molecules/cm^2 and 4×10^{14} molecules/cm^2 respectively) from about 3.0ML to 7ML ZnO_x (coverage determined by AES). A diffuse (1×1) LEED pattern due to the copper substrate can still be observed at ≈7ML ZnO_x. At coverages above 7ML, the ZnO_x islands begin to collapse as evidenced by an increase in CO_2 adsorption capacity. The diffuse (1×1) LEED pattern does not completely disappear until >8ML ZnO_x, and evidence of bare Cu(110) as detected by CO adsorption remains until >15ML ZnO_x.

5 Discussion

We have seen evidence of some of the complexities anticipated in attempting to grow ZnO_x overlayers on copper single crystals; oxygen adsorption onto copper as well as zinc oxide formation, diffusion of oxygen into and out of bulk copper, and so on. We have also seen an additional complication of rapid clustering of ZnO_x into three-dimensional islands at temperatures above 300K. Hence, to avoid three-dimensional islands, we evaporated zinc in an oxygen ambient at 150K.

Ideally, we would like an ordered ZnO overlayer on copper. Examining the unit cells of various zinc oxide and copper single crystals, the best fit is between ZnO($10\bar{1}0$) and Cu(110): For Cu(110), a=3.61 $\AA$, b=2.55 $\AA$, and for ZnO($10\bar{1}0$), a=3.2495 $\AA$, b=5.2069 $\AA$. There is a 10% mismatch between the Cu(110) and ZnO($10\bar{1}0$) faces for one side of their unit cell, and taking twice the distance of b=2.55 $\AA$ for Cu(110) (so the overlayer is a p(2×1)), there is a 2% mismatch between the other side of the two faces. Hence, by requirement of similar unit cell dimensions, ordered ZnO layers on Cu(110) seemed plausible. But we have seen that even with an initial p(2×1)O/Cu(110), the resulting ZnO_x overlayer produced no long range order.

We have seen that by depositing zinc vapor and oxygen onto Cu(110), a surface species forms which adsorbs CO_2. This indicates the formation of zinc oxide. The temperature at maximum rate of desorption of CO_2 from this ZnO_x surface is 510K, 170K higher than from submonolayers to multilayers of ZnO_y on gold foils. This shift in binding energy may be due to interactions between copper and zinc oxide or it may be due to the structure of the ZnO_x overlayer on Cu(110). Reports in the literature have shown CO_2 desorption to occur between T_p=350K and 400K for ZnO single crystal orientation of ($10\bar{1}0$), ($40\bar{4}1$), and ($50\bar{5}1$)[8,18]. In contrast, the polar ZnO single crystal of (0001) orientation interacts with CO_2 more strongly, as indicated by the maximum rate of desorption of 670K[18]. Hence, the difference in binding energy of CO_2 on the three-dimensional ZnO_x islands/Cu(110) and on ZnO_y/Au may be due to differences in the overlayer structure (i.e. dipole moment and defect density).

We have noted that the temperature of peak desorption changes for CO_2 from the two-dimensional ZnO_x islands to the three-dimensional islands. For example, the highest T_p for the two-dimensional ZnO_x overlayer is at 510K while for the three-dimensional ZnO_x islands, the highest T_p is at 550K. This is most likely due to different faces of ZnO exposed in the two different cases. With additional annealing, we obtained more and more CO_2 adsorption indicative of non-polar faces of ZnO (T_p=340K).

While we have observed various CO_2 desorption peaks depending on preparation of

the surface, CO desorption is always a narrow peak centered at T_p=218K except when the copper is covered with $\geq$0.4ML oxygen. It may be surprising that ZnO_x islands have no influence on the binding energy of CO to Cu(110), but this insensitivity of CO adsorption on copper has been previously seen for CO adsorption on cobalt modified Cu(100)[19].

It would be interesting to observe the interaction of copper, zinc, and oxygen by STM in the barrier height mode; the initial two-dimensional structures, the three-dimensional island formation upon heating above 300K, and changes in structure and composition upon further oxygen and heat treatments.

6 Conclusion

It is possible to grow two-dimensional ZnO_x islands on Cu(110), but these islands cluster into three-dimensional islands above 300K. These three-dimensional ZnO_x islands do not adsorb detectable amounts of CO_2 because of oxygen deficiency. Once these oxygen deficient ZnO_x islands are oxidized, CO_2 adsorption capacity increases to detectable levels. Carbon dioxide chemisorption properties on three-dimensional islands vary depending upon heat treatments. At first, strong adsorption associated with polar faces and/or defect sites are observed. With increasing heat treatments at 700K, adsorption indicative of non-polar faces of ZnO increases.

Carbon monoxide adsorption on Cu(110) is unaffected by the presence of ZnO_x. Hence, CO titration can be used to determine the amount of exposed Cu(110). From a combination of CO and CO_2 titrations, it appears that zinc oxide prefers to grow as three-dimensional islands on Cu(110). These ZnO_x islands do not collapse until AES indicates >7ML ZnO_x. Heating in vacuum and in oxygen failed to spread these islands onto the copper substrate.

Acknowledgement

The authors would like to thank Miquel B. Salmeron for many helpful discussions. This work was supported by the Director, Office of Energy Research, Office of Basic Energy

Sciences, Materials Sciences Division, of the U.S. Department of Energy under Contract No. DE-AC03-76SF00098.

References

[1] R.G. Herman, K. Klier, G.W. Simmons, B.P. Finn, and J.B. Bulko, J. Catal. 56 (1979) 407.

[2] J.A. Rodriguez and C.T. Campbell, J. Phys. Chem. 91 (1987) 6648.

[3] C.T. Campbell, R.A. Daube, and J.M. White, Surface Sci. 182 (1987) 458.

[4] K.L. Siefering and G.L. Griffin, Surface Sci. 207 (1989) 525.

[5] L. Chan and G.L. Griffin, Surface Sci. 173 (1986) 160.

[6] S.V. Didziulis, K.D. Butcher, S.L. Cohen, and E.I. Solomon, J. Am. Chem. Soc. 111 (1989) 7110.

[7] E. Giamello, B. Fubini, and V. Bolis, Applied Catal. 36 (1988) 287.

[8] W. Hotan, W. Gopel, and R. Haul, Surface Sci. 83 (1979) 162.

[9] J. Nakamura, J.A. Rodriguez, and C.T. Campbell, J. Phys. Condensed Matter. 1SB (1989) 149.

[10] K. Horn, M. Hussain, and J. Pritchard, Surface Sci. 63 (1977) 244.

[11] G. Ertl, Surface Sci. 6 (1967) 208.

[12] G.W. Simmons, D.F. Mitchell, and K.R. Lawless, Surface Sci. 8 (1967) 130.

[13] L. Chan and G.L. Griffin, J. Vac. Sci. Technol. A3(3) (1985) 1613.

[14] C.R. Brundle and R.I. Bickley, J. Chem. Soc. Faraday Trans. II 75 (1979) 1030.

[15] I. Wach and R. Madix, J. Catal. 53 (1978) 208.

[16] D. Kohl, M. Henzler, and G. Heiland, Surface Sci. 41 (1974) 403.

[17] C.T. Au, W. Hirsch, and W. Hirschwald, Surface Sci. 197 (1988) 391.

[18] W.H. Cheng and H.H. Kung, Surface Sci. 122 (1982) 21.

[19] F. Falo, I. Cano, and M. Salmeron, Surface Sci. 143 (1984) 303.

Figure Captions

Figure 1. Schematic drawing of some of the species possible in Cu-Zn-O interaction on Cu(110).

Figure 2. Desorption of 0.1ML zinc adsorbed on Cu(110); a) clean Cu(110), b) 0.5ML oxygen preadsorbed on Cu(110), c) same as b but zinc dosed in 1×10^{-7} Torr O_2 ambient, and d) same as c with additional oxidation in 5×10^{-7} Torr O_2 for 20 minutes at 300K. All zinc and oxygen depositions were done at 300K. Similar results are obtained for zinc and oxygen depositions at 150K. AES shows a peak at 988eV for all these surfaces except for zinc on clean copper (i), which has its LVV transition at 992eV. No zinc could be detected by AES after each TPD ending at 1100K. As reference, zinc desorption from multilayers of pure zinc and zinc desorption from ZnO(0001)[16] are shown. The zinc desorption from ZnO(0001)[16] is not on the same scale as the rest of the data. As in all TPD spectra shown throughout this paper, each TPD spectrum is offset by a certain amount from the rest for better viewing. For example, curve (ii) does not have a higher background than curve (i) but is just offset by a value of 8 arbritrary units.

Figure 3. (i) AES intensities of Cu, Zn, and O peaks vs. zinc deposition time. Zinc was dosed in 1×10^{-7}Torr O_2 at 150K. Arrow points to copper AES intensity from clean Cu(110). By depositing 0.5ML oxygen onto Cu(110), the copper 918eV AES signal attenuates by 10%. (ii) Accompanying saturation CO_2 adsorption for each coverage in (i). From the CO_2 adsorption versus zinc and oxygen deposition time, monolayer completion occurs after 20 minutes deposition time. Each surface is prepared fresh from 0.5ML O/Cu(110).

Figure 4. (ia) CO TPD from a freshly prepared surface of 1.0ML ZnO_x on Cu(110) and (ib) CO_2 TPD from a freshly prepared surface of 1.0ML ZnO_x on Cu(110). (ii) After

the first TPD; (a) saturation CO adsorption is now 100% of that from clean Cu(110), and (b) the surface no longer adsorbs CO_2. The third, the fourth, the fifth, etc. TPD spectrum are all exactly like (iia) and (iib). The CO_2 spectra are offset from the CO spectra for clearer viewing. There is no visible order by LEED for the freshly prepared surfaces. After the first TPD, LEED shows a diffuse (1×1) pattern.

Figure 5. CO and CO_2 adsorption capacity vs. pre-annealing temperature of the ZnO_x overlayer on Cu(110). Each experiment requires the preparation of a fresh surface since above 300K the ZnO_x/Cu(110) surface changes.

Figure 6. Effect of annealing on Zn TPD: a) 0.8ML ZnO_x, b) same as (a) but annealed at 670K for 5 minutes before Zn TPD, and c) same as (b) but annealed for 10 minutes at 670K.

Figure 7. (i) Chemisorption of surface produced after surface represented in figure 4(ii) was exposed to 5×10^{-7} Torr O_2 for 10 minutes at 300K and annealed at 700K for 2 seconds. (ii) CO and CO_2 desorption spectra after an additional exposure of 5×10^{-7}Torr O_2 for 10 minutes at 300K. All TPD data were obtained from saturation coverages of CO or CO_2. Surfaces which give CO_2 desorption spectra similar to figure 7 contain the highest zinc desorption peak (peak d of figure 2) in their zinc TPD spectra. LEED shows diffuse p(2×1) patterns throughout these oxygen treatments.

Figure 8. Effect of annealing at 700K on CO_2 chemisorption properties: a) 3.0ML ZnO_x/Cu(110), b) after annealing (a) to 700K for 2.0 minutes, and c) after an additional 10 minutes anneal at 700K.

CO and CO_2 Desorption from Various Surfaces
(Adsorption at 150K)

Surfaces	CO T_p	CO $\theta_{sat.}$	CO_2 T_p	CO_2 $\theta_{sat.}$
Cu(110)	218K	0.5ML	no ads.	—
0.5ML O/Cu(110)	222K & 180K	<0.05ML	no ads.	—
Cu_xO	222K & 180K	<0.03ML	no ads.	—
Zn	no ads.	—	no ads.	—
ZnO_y	203K	<0.05ML	340K & 175K	0.2ML

a. Each surface prepared as described in the experimental section.

b. T_p=temperature at peak desorption and $\theta_{sat.}$=saturation coverage where θ=1 is defined as 1.1×10^{15} molecules/cm^2 corresponding to the number of copper atoms on the Cu(110) surface.

Table 1

Effect of Co-Adsorption on CO & CO_2 Adsorption Capacity

Treatment	Amount of CO desorbed molecules/cm^2	Amount of CO_2 desorbed molecules/cm^2
3L CO_2 then 2L CO	4.1×10^{14}	9.0×10^{13}
2L CO alone	$4.0\pm0.1\times10^{14}$	———
2L CO then 3L CO_2	3.9×10^{14}	8.8×10^{13}
3L CO_2 alone	———	$8.7\pm0.3\times10^{13}$

Table 2

Summary of AES, LEED, and CO & CO_2 TPD data for 3.0ML ZnO_x/Cu(110) annealed at 700K

Surface	AES Intensities (Arb. Units) Cu Zn O	LEED Pattern	CO Adsorption Capacity (molecules/cm^2)	CO_2 Adsorption Capacity from T_p=340K (molecules/cm^2)	Amount of CO_2 from all other desorption peaks (molecules/cm^2)	Total CO_2 Adsorption Capacity (molecules/cm^2)
(a) "3.0ML ZnO_x"*	39 10 40	(1×1)	4.0×10^{14}	$<3\times10^{11}$	9.0×10^{13}	9.0×10^{13}
(b) After 700K/2.0 min.	39 6.7 32	(1×1)	4.1×10^{14}	1.4×10^{13}	6.1×10^{13}	7.5×10^{13}
(c) After an additional 700K/10.0 min.	39 6.0 32	diffuse p(2×1)	1.2×10^{14}	2.9×10^{13}	4.4×10^{13}	7.3×10^{13}

*Coverage determined by AES

Table 3

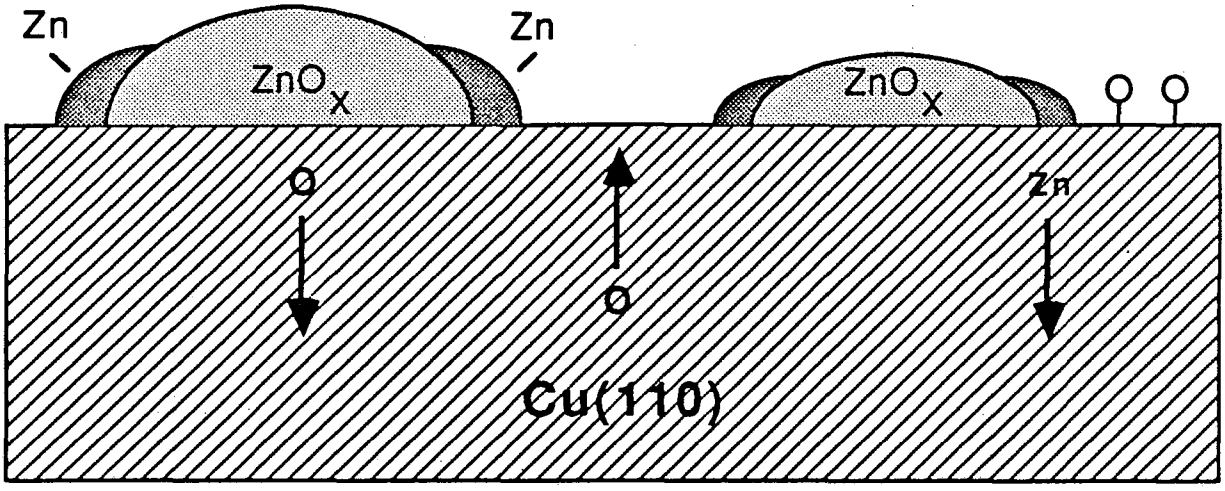

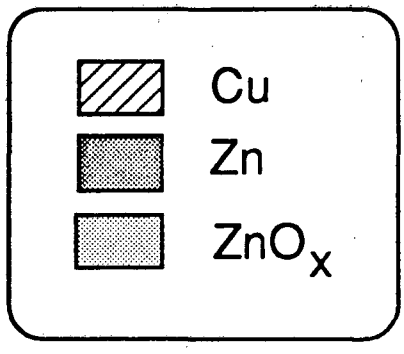

Fig. 1

XBL 904-1413

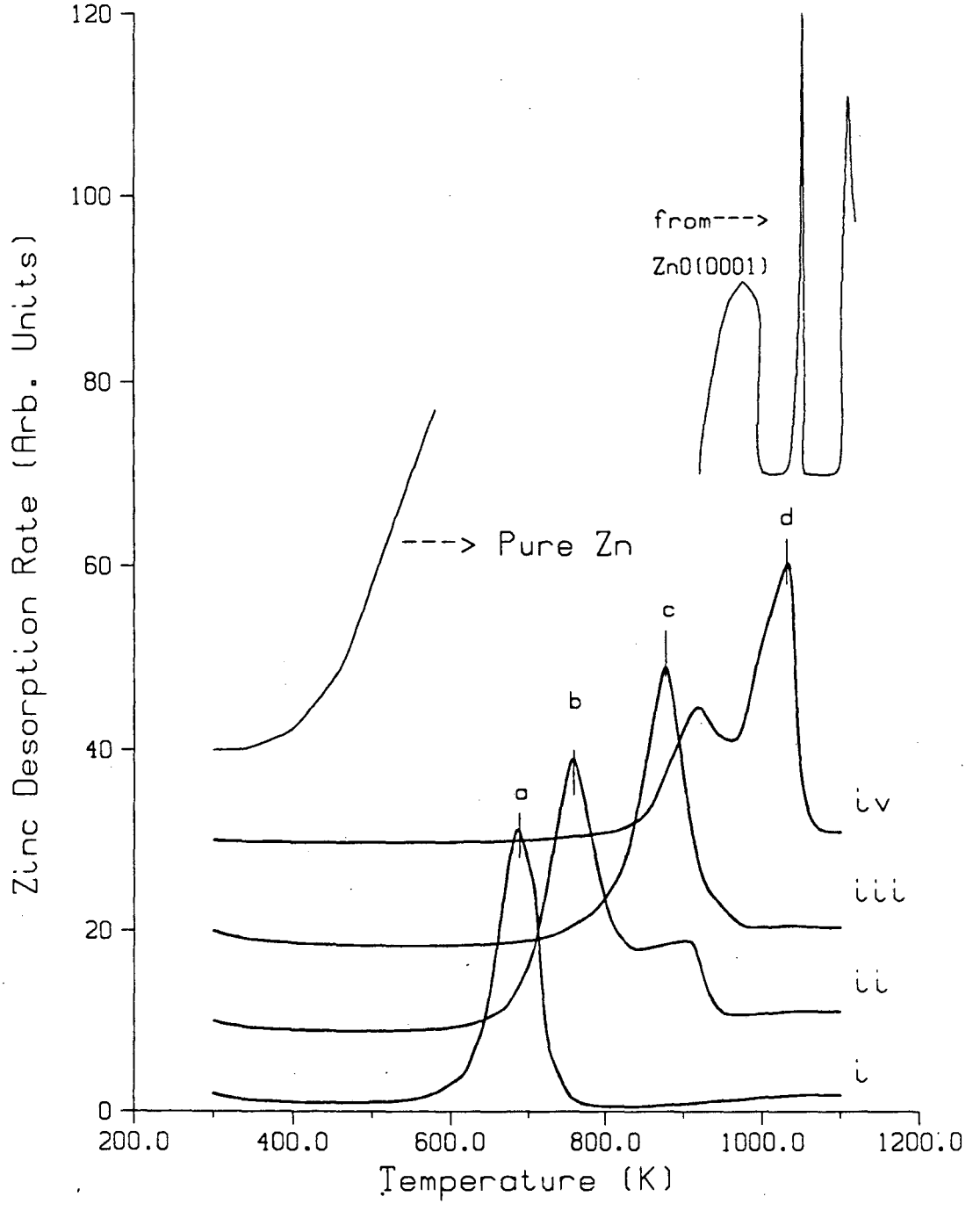

XBL 904-1411

Fig. 2

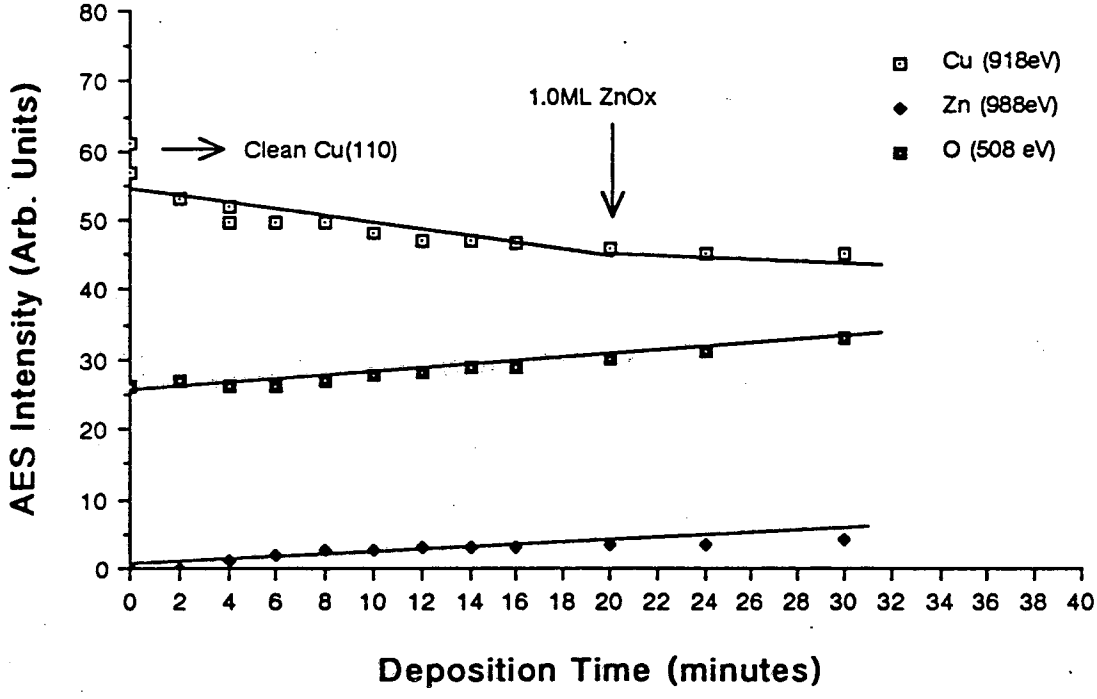

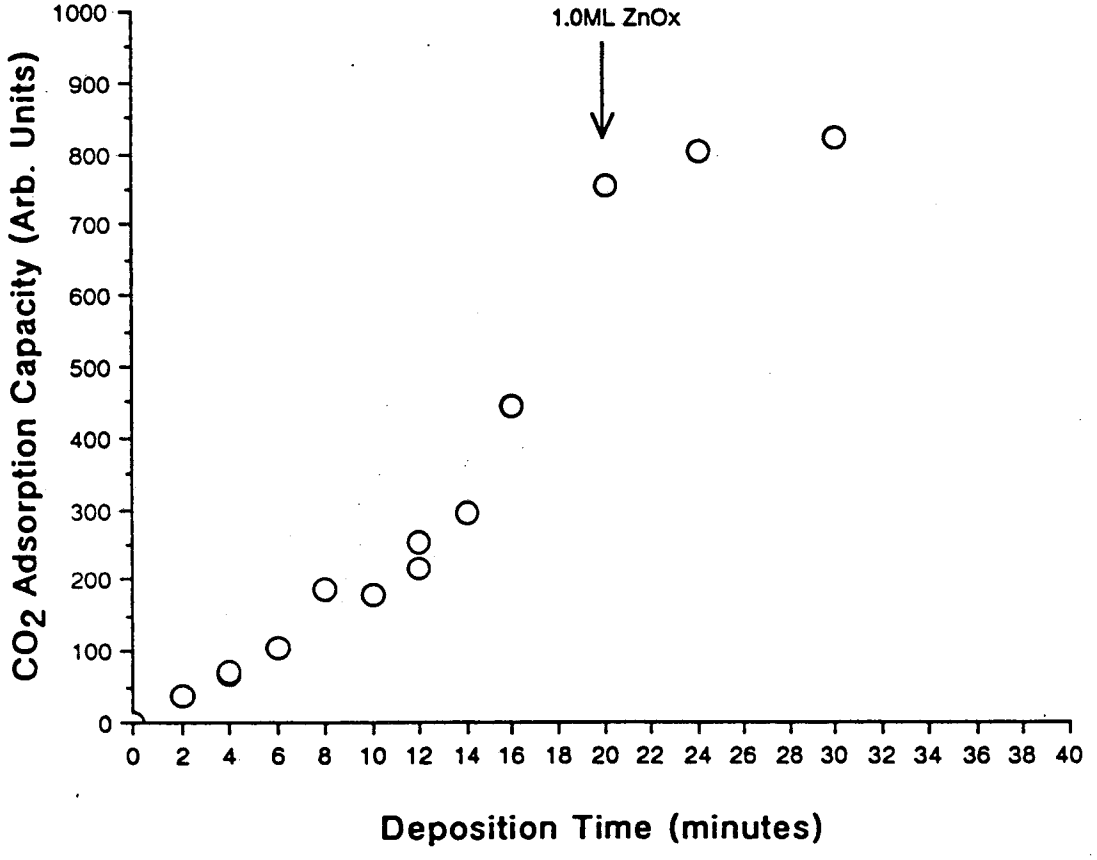

XBL 904-1408

Fig. 3

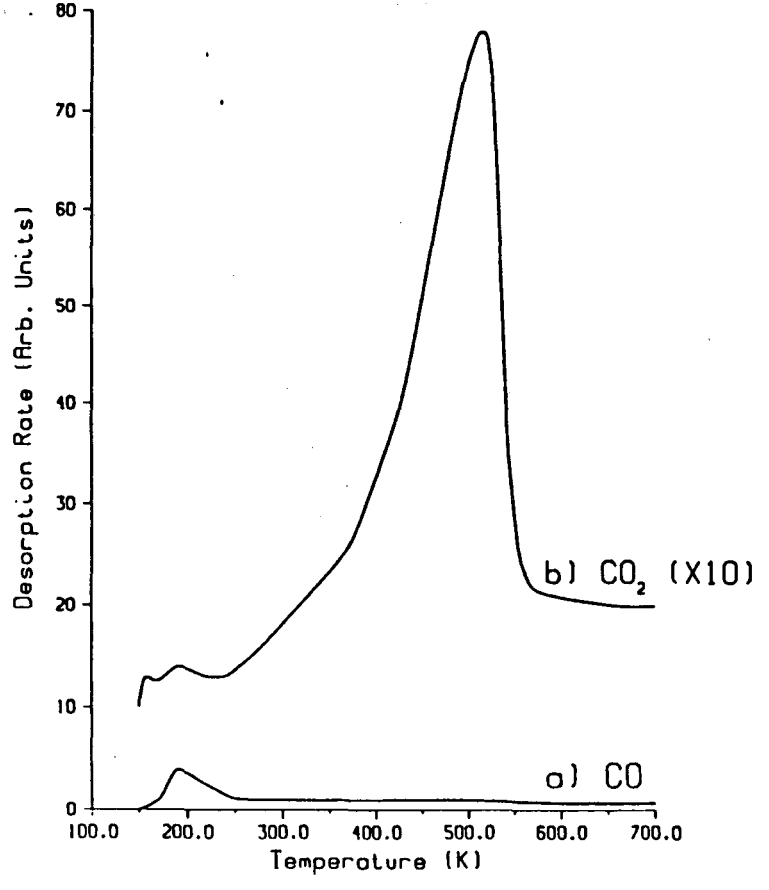

Fig. 4(i)

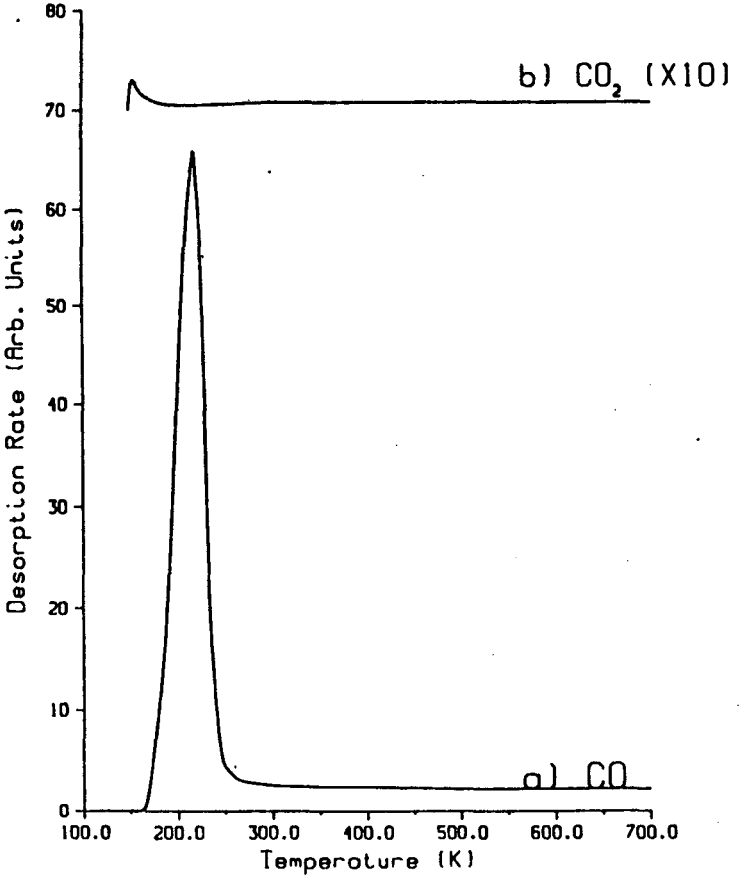

XBL 904-1410

Fig. 4(ii)

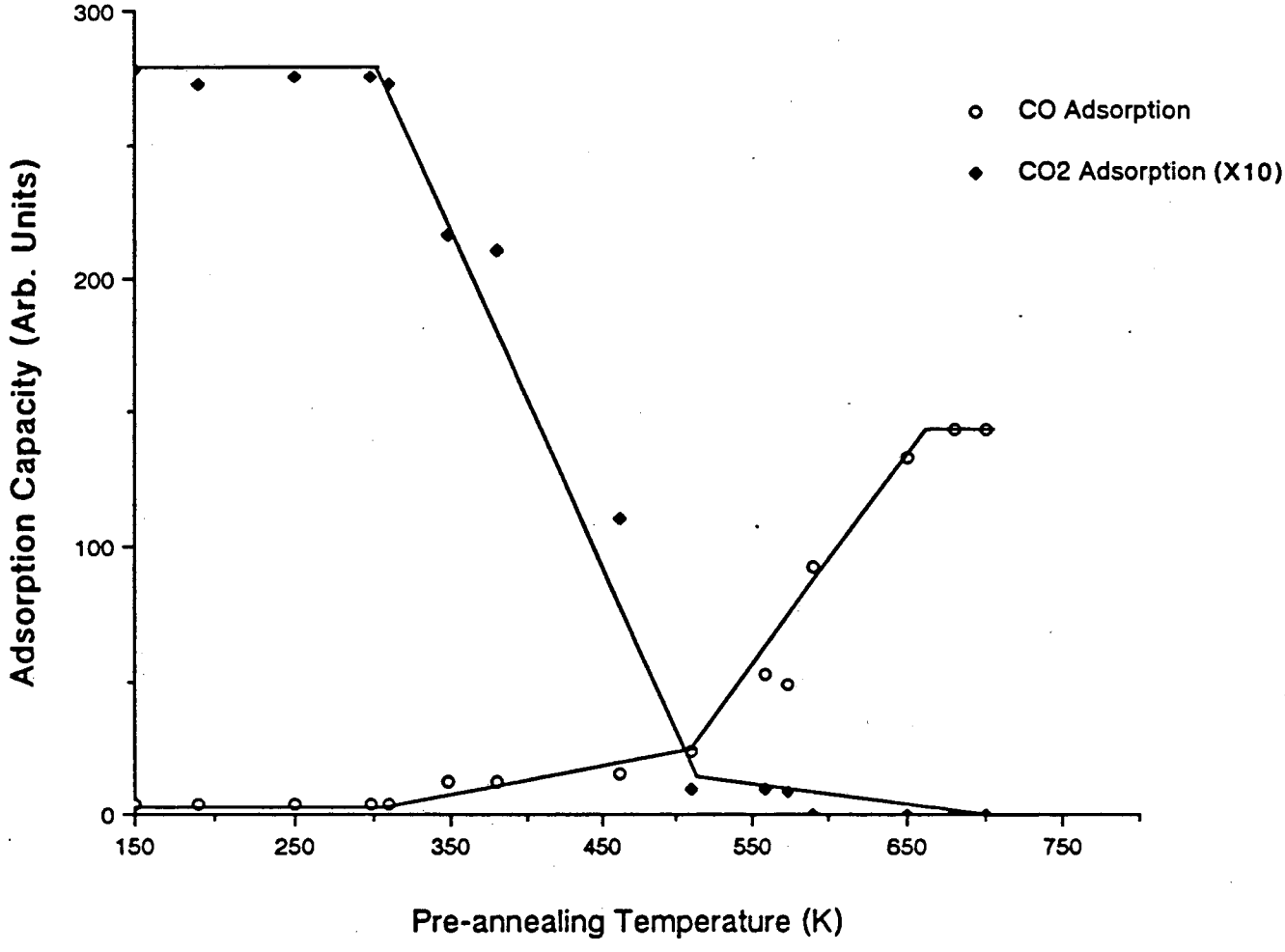

XBL 904-1414

Fig. 5

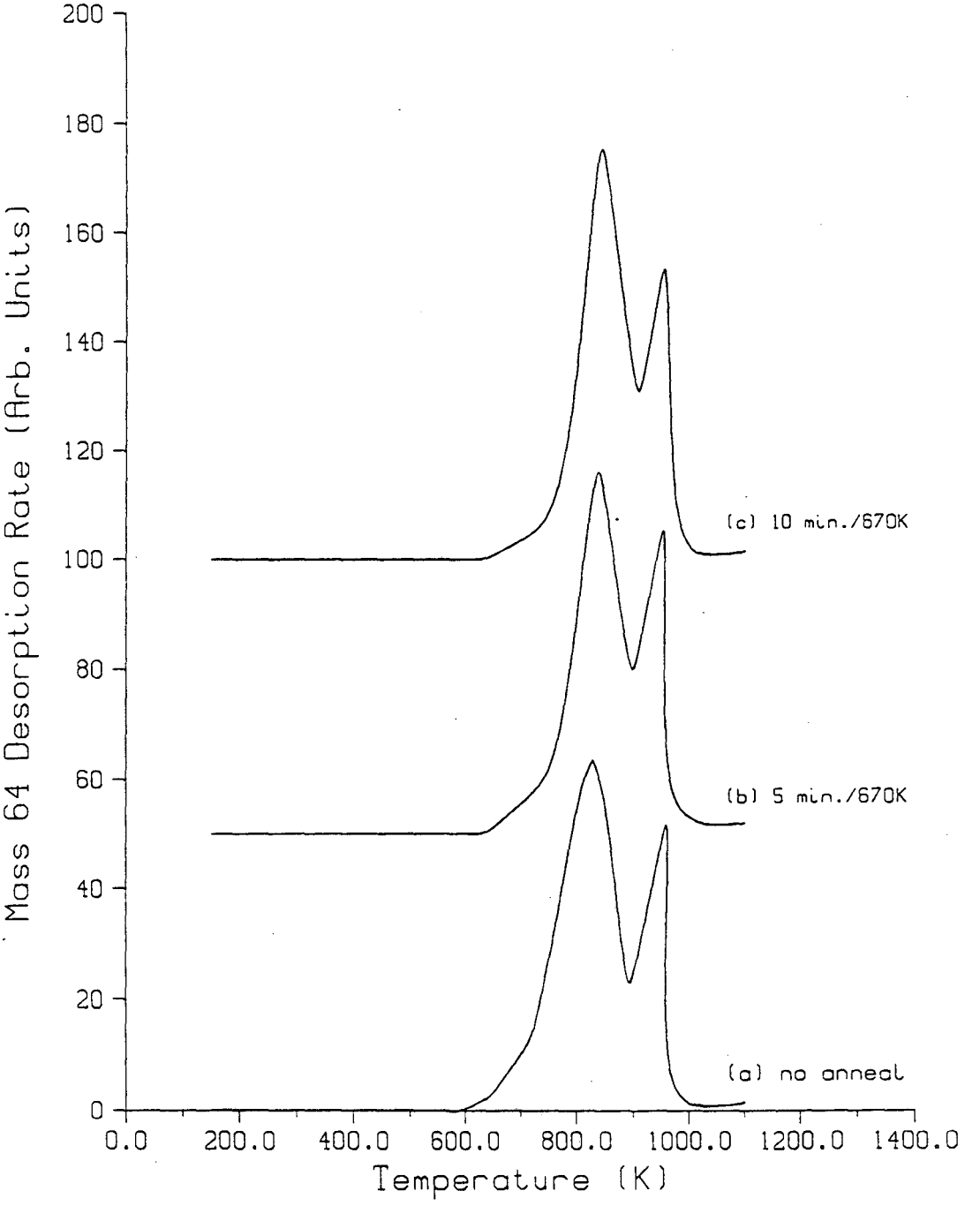

XBL 904-1412

Fig. 6

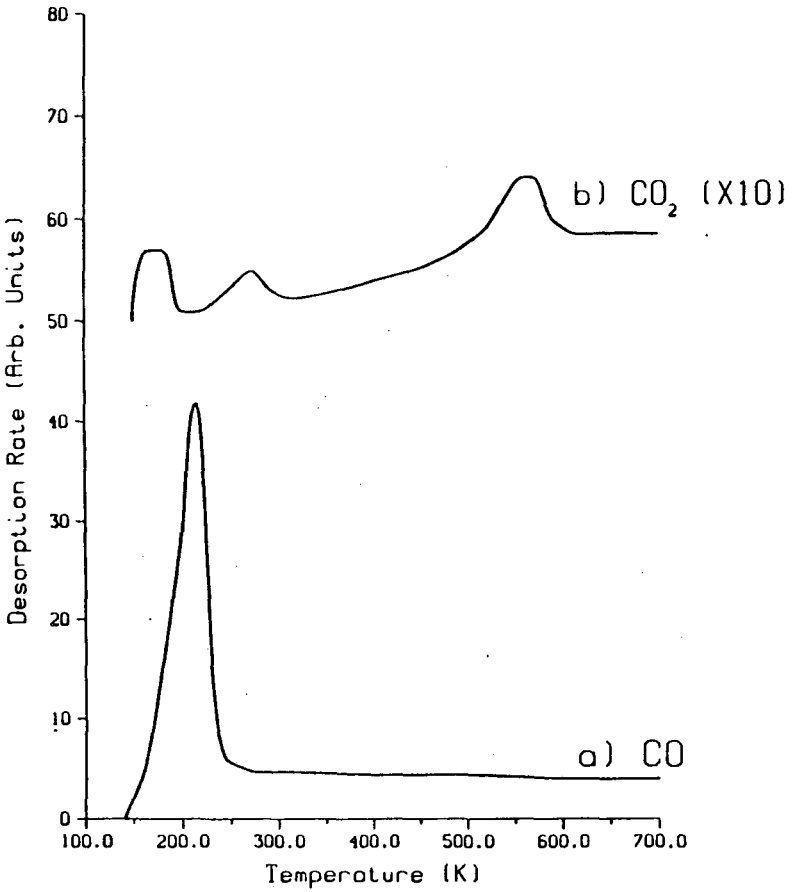

Fig. 7(i)

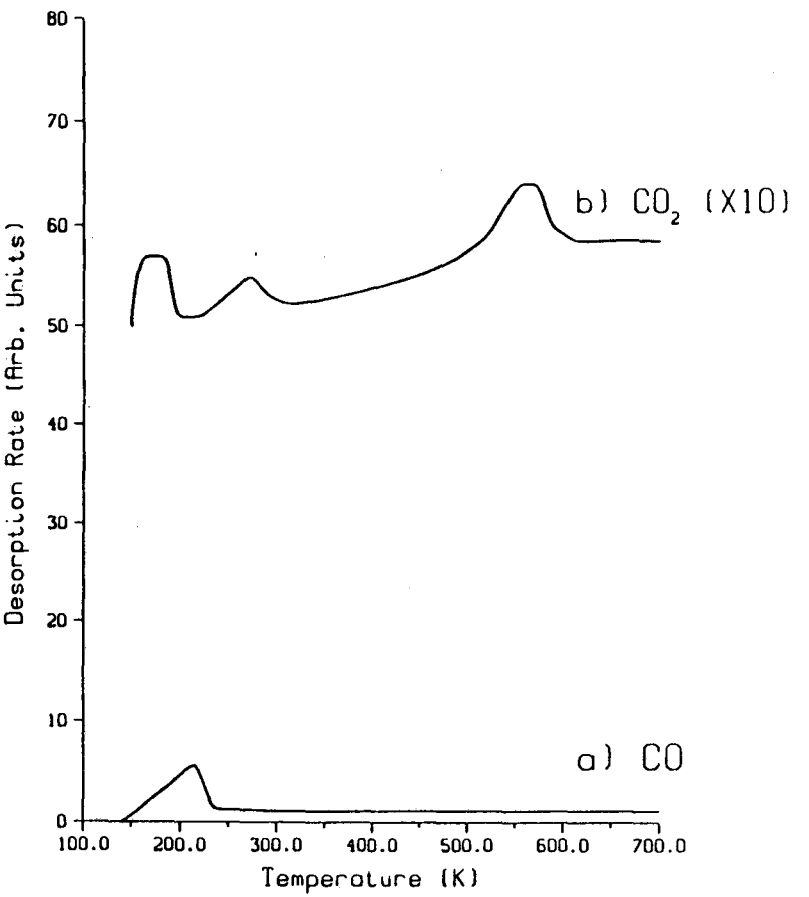

XBL 908-2790

Fig. 7(ii)

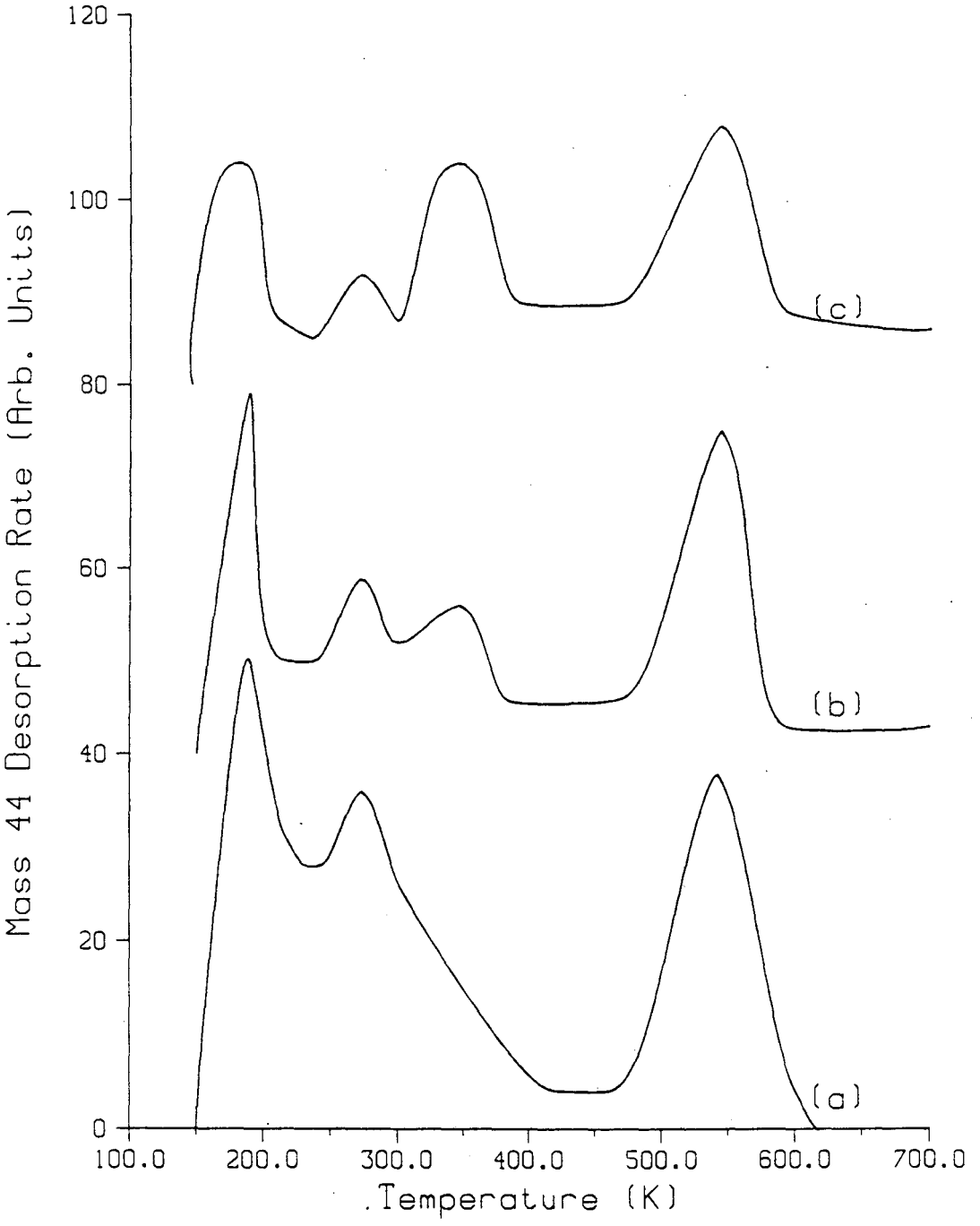

XBL 904-1415

Fig. 8

LAWRENCE BERKELEY LABORATORY
CENTER FOR ADVANCED MATERIALS
1 CYCLOTRON ROAD
BERKELEY, CALIFORNIA 94720